EEG Activities of Dynamic Stimulation in VR Driving Motion Simulator

Chin-Teng Lin[1,3], Li-Wei Ko[1,3], Yin-Hung Lin[1], Tzyy-Ping Jung[1,2], Sheng-Fu Liang[1,4], and Li-Sor Hsiao[1,3]

[1] Brain Research Center, National Chiao-Tung University (NCTU), Hsinchu 300, Taiwan, R.O.C

[2] Swartz Center for Computational Neuroscience, Institute for Neural Computation, University of California, San Diego, USA

[3] Department of Electrical and Control Engineering, National Chiao-Tung University (NCTU), Hsinchu 300, Taiwan, R.O.C

[4] Department of Computer Science and Information Engineering, National Cheng Kung University, Tainan 701, Taiwan, R.O.C

Abstract. The purpose of this study is to investigate Electroencephalography dynamics in response to kinesthetic stimuli during driving. We used a Virtual Reality driving simulator consisted of a hydraulic hexapod motion platform to create practical driving events. We compared the EEG dynamics in response to kinesthetic stimulus while the platform was in motion, to that while the platform was stationary. The scalp-recorded EEG channel signals were first separated into independent brain sources using Independent Component Analysis (ICA), and then studied with time-frequency analysis. Our results showed that independent brain processes near the somatomotor cortex exhibited alpha power decreases across sessions and subjects. Negative potentials phase-locked to the onsets of deviation events under motion conditions were observed in a central midline component. The results allow us to better understand different brain networks involved in driving, and provide a foundation for studying event-related EEG activities in the presence of kinesthetic stimuli.

Keywords: Kinesthetic Stimulus, EEG, ICA, Component Clustering, ERSP, ERP, Mu Rhythm, EMG.

1 Introduction

Kinesthetic perception -- the sensory apparatus that detects motion -- is one of the most important sensations to human beings, yet we usually overlook the contributions of the vestibular system to our lives. However, we would not have a complete sensation of the world without the perception of motion. We cannot even stand still or walk in a straight line without the vestibular system functioning properly. The vestibular system thus plays an important role in our lives.

Researchers have tried to measure evoked potentials of vestibular origin for 30 years. Elidan et al. [1] reported the ERP response to high speed and transient vertical Z axis rotation. Subjects were rotated at the speed of 10,000°/sec2 for 2 ms. The

D. Harris (Ed.): Engin. Psychol. and Cog. Ergonomics, HCII 2007, LNAI 4562, pp. 551–560, 2007.

reported negativity peaked at about 15 ms after the onsets of rotation from signals measured at a forehead mastoid electrode. Baudonniere et al. [2] reported a biphasic negative wave, that is most prominent at central midline electrode (Cz) in subjects who received short (30 ms) linear displacements without co-stimulation of the semicircular canals.

Probst et al. [3-5] and Loose et al. [6] observed bell-shaped negativity at central midline channels following roll up and down motion along the X axis. The Vestibular Evoked Potential (VESTEP) evoked by stimulating otolithic and semicircular canals with different orientations of rotations or directions of movements was investigated in depth.

The experimental variables in these studies were well controlled. This might be desirable from the perspective of scientific research, but is less practical because we rarely experience vestibular stimulation without visual co-stimulation or watch pixels rotating or moving in the real world. We actually live in a visual-vestibular co-stimulation world and the visual cue is always a meaningful and continuous scene -- in driving, for instance.

The driving perception includes the co-stimulation of visual cue, vestibular stimulation, muscle reaction, and skin pressure. This is indeed a complicated mechanism to understand.

Using a realistic simulator to conduct driving experiments is widely used in driving-related research [7]. Regarding the necessity of motion during driving, the literature shows that the absence of motion information increases reaction times to external movement perturbations [8], and decreases safety margins in the control of lateral acceleration in curve driving [9]. In real driving, improper signals from disordered vestibular organs were reported to contribute to inappropriate steering adjustment [10]. Groen et al. [11] also showed that the presence of vestibular information in driving simulators was important in the perception of illusory self-tilt and illusory self-motion. These studies emphasized the importance of motion perception during driving to the assessment of driving performance and behavior.

The electroencephalogram (EEG) is a popular method for evaluating human cognition. Compared to functional Magnetic Resonance Imaging (fMRI), EEG is much less expensive and more portable, thus it is applicable in our daily lives, especially on the move.

In recent years, researchers have designed the Virtual Reality (VR) scenes to provide appropriate environments for assessing brain activity during driving [12-14]. Lin et al. [12,13] introduced the “dynamic” VR environment in conjunction with physiological and behavioral response recordings to offer more assessment options than were available in traditional neuropsychological studies. However, the EEG correlates of kinesthetic stimulations induced by the motion platform in the dynamic VR scene have not been fully assessed or appreciated.

The purpose of this study is to investigate EEG dynamics in response to kinesthetic stimuli using a dynamic VR environment. To this end, we constructed an interactive driving environment that integrated a surrounding scene and a real vehicle mounted on a hydraulic hexapod motion platform. This dynamic VR environment mimicked visual-vestibular co-stimulation during driving. Using simple driving behaviors, we studied brain responses of kinesthetic inputs by comparing subjects’ EEG differences in motion and motionless conditions of the dynamic platform.

2 Material and Methods

We developed a VR-based 3D high-fidelity interactive highway scene. The synchronized scenes were projected from seven projectors to constitute a surrounding vision. At the center of the projected scenes, a real vehicle mounted on the motion platform to provide motion sensations. The vestibular cues were delivered by a Stewart Platform [15]. The platform generated accelerations in vertical, lateral, and longitudinal directions of a vehicle as well as pitch, roll, and yaw angular accelerations. This technique has been used widely in driving simulation studies [16].

We designed three driving events: stop, go, and deviation. Figure 1 shows the time course of a typical Stop-Go event. Subjects did not need to do anything in the events. Moreover, the vehicle was randomly drifted away from the cruising position, and the subjects were instructed to steer the vehicle back to the center of the cruising lane as quickly as possible (Figure 2).

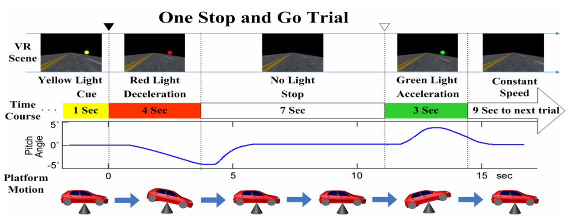

Fig. 1. Illustration of the design for Stop-Go events in driving

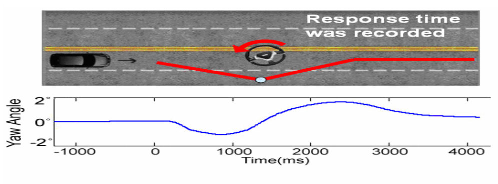

Fig. 2. The vehicle was randomly drifted away from the cruising position, which was defined as a deviation event, and the subjects were instructed to steer the vehicle back to the center of the cruising lane as quickly as possible

Ten healthy subjects participated in this research (aged between 20 and 28). Subjects were instructed to keep the car at the center of the inside lane by controlling the steering wheel, and to perform the driving task consciously. Each subject completed four 25-minute sessions in each driving experiment. The entire driving experiment lasted about 2 hours. Subjects performed at least 2 driving experiments on different days for testing the cross-session consistency.

The physiological data acquisition uses 33 unipolar sintered Ag/AgCl EEG/EOG electrodes and 2 bipolar ECG electrodes placed on the chest. All the EEG/EOG electrodes were placed based on a modified International 10-20 system and refer to the right ear lobe. The contact impedance between EEG electrodes and scalp was calibrated to be less than 5kΩ. We used the Scan NuAmps Express system

(Compumedics Ltd., VIC, Australia) to simultaneously record the EEG/EOG/ECG data and the deviation between the center of the vehicle and the center of the cruising lane triggered by the VR program. The EEG data were sampled at 500 Hz with a 16-bit quantization level.

The continuous EEG signals were first extracted into epochs whose lengths were designed to cover the whole platform dynamics in single driving events. We then applied Independent Component Analysis to concatenated epochs to decompose them into temporally statistical component activations.

ICA methods have been extensively applied to the blind source separation problem since the 1990s [17-21]. Subsequent technical reports [22-28] demonstrated that ICA was a suitable solution to the problem of EEG source segregation, identification, and localization.

To study the cross-subject component stability of ICA decomposition, components from multiple sessions and subjects were clustered based on their spatial distributions and EEG characteristics [24], [29].

Component Clustering grouped massive components from multiple sessions and subjects into several significant clusters and identified at least 9 clusters of components having similar power spectra and scalp projections. These component clusters also showed functionally distinct activity patterns.

Single-trial event-related potential (ERP) data are usually averaged prior to analysis to increase their signal/noise relative to non-time and -phase locked electroencephalographic (EEG) activity and non-neural artifacts.

Event-Related Potential (ERP) images directly visualized single event-related EEG trials and their contributions to the averaged ERP [24]. An ERP image also makes visible relationships between subject behavior and amplitudes/latencies of individual event-related responses.

Event-Related Spectral Perturbation (ERSP) plots the grand mean time course of changes from pre-stimulus baseline in log spectral power of a scalp-recorded EEG or ICA component activation time-locked to stimulus presentation or subject responses across frequencies. Through ERSP, we are able to observe time-locked but not necessarily phase-locked activities [30].

3 Results

3.1 Mu Component Activations

Figure 3 shows the ERSP of a component that exhibited differential brain responses between motion and motionless conditions. The component scalp map exhibited the defining features of mu rhythms -- distinct spectral peaks near 10 Hz and 22 Hz. The upper ERSP panels show the ERSP following stop events, while the lower two show go-event ERSP. Images on the left are brain responses under “motion” conditions and those on the right are under “motionless” conditions. The curves below the images are the time courses of the platform motion (pitching, rotate by Y axis). Mu power was strongly blocked (reduced) around the peak of platform motion in Motion-Stop and Motion-Go events. In contrast, no mu blocking occurred following either stop or go events in the motionless condition (Fig. 3, right panels). Thus the mu blocking appears to be induced by the kinesthetic inputs in stop and go events.

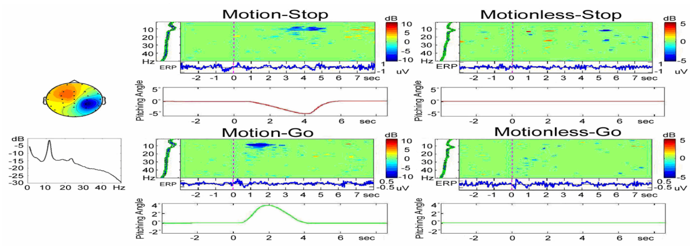

Fig. 3. A right mu component shows mu characteristic 10 Hz and 22 Hz peaks in the activity spectrum (lower left). The component mean ERSP shows mean event-related changes in (log) spectral power across data trials time-locked to the kinesthetic stimulus onsets (dashed line). Following the motion platform movement, this activity is blocked. The activity was unchanged from the baseline spectra if the motion platform was not in action (right).

Mu blocking was also observed following deviation events. Figure 4 shows the ERSP of a right mu component following deviation events. The upper and lower panels show ERSPs of the component following “deviate-to-left” and “deviate-to-right” events, respectively. The curves below show the motion recordings of the platform. Notice that the motion platform tilted along different directions in Stop-Go and deviation events (cf. Fig. 3). In deviation events, the platform rotated slightly along the vertical Z axis.

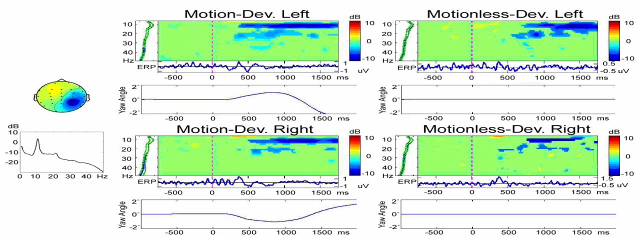

Fig. 4. The mean ERSP of the mu component follow deviation events

When deviation occurred, the subjects were instructed to maneuver the car back to the cruising position by steering the wheel. It is expected that mu activity would be blocked due to the hand movement in both motion and motionless conditions. However, the latency of mu blocking in the motion condition was significantly shorter than that in the motionless condition.

3.2 Central Midline (CM) Component Activations

Figure 5 shows the scalp map and dynamic properties of an independent component from the same subject in Motion-Deviation and Motionless-Deviation conditions. The scalp map of the CM component (Fig. 5 upper left) resembles scalp maps of the “P3a” or “P3novel” ERP peaks [31-32]. In two-dimensional “ERP image” plots of single trials from the subject, potential fluctuations are shown as color-coded horizontal lines, here normalized by component activation baseline variability then sorted by response time (RT). The ERP images clearly show that the early kinesthetic response,

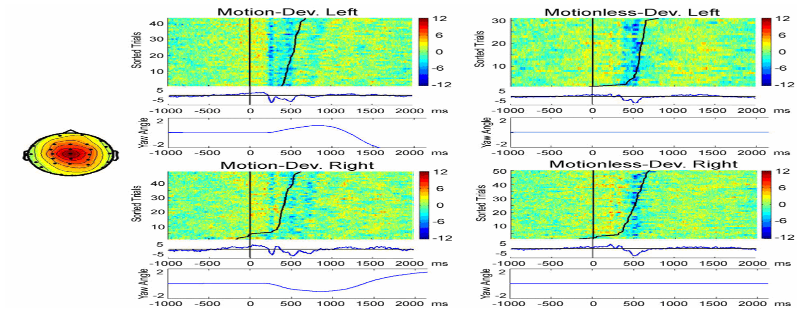

Fig. 5. Single-trial Event-Related Potentials (ERPs) of the central midline (CM) component

peaked at ~250 ms, was time-locked to deviation onset. However, this sharp negativity was missing in the motionless condition (Fig. 5 right panels).

3.3 Component Stability

There were 29 components from 10 subjects contributing to a large cluster of left mu components. We found that the 11 Hz activity was blocked following kinesthetic stimuli in the motion condition. Hence, we strongly suggested that these represented mu activity [33]. Scalp maps of individual left mu components in this cluster strongly resembled the cluster mean map.

Figure 6a shows the component cluster mean ERSP of the component activations following Stop-Go events under the motion and motionless conditions. The ERSP images of motion sessions exhibited a strong mu blocking and alpha rebound, which were completely missing from the ERSP images under motionless conditions, consistent with the results in a typical subject shown in Figure 3.

Similarly, Figure 6b shows averaged ERSP images following deviation events under motion and motionless conditions. Although the ERSP images in all four conditions exhibited similar mu blocking induced by the steering actions, the latencies of mu blocking differed considerably.

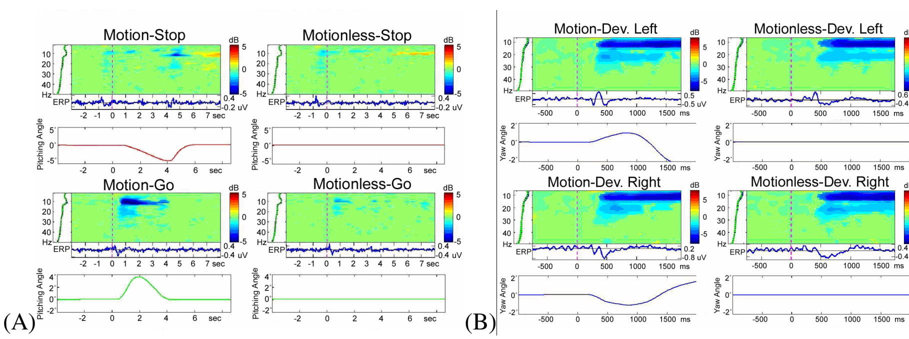

Fig. 6. (A) The group-averaged ERSP shows the component activations following Stop-Go events under the motion (left panels) and motionless (right panels) conditions. (B) The group-averaged ERSP images following deviation events under motion and motionless conditions.

4 Discussions

In this study, we recorded and analyzed unaveraged single-trial EEG data in 31 driving experiments from 10 volunteer drivers under two different driving conditions -- motion and motionless. The hexapod motion platform that simulated driving events allowed us to study neural correlates of kinesthetic stimuli. We performed ICA to separate the EEG contributions of distinct brain processes to explore their individual and joint event-related dynamics following Stop-Go and deviation events through ERP differences and time-frequency analysis (ERSP). Alpha power of the mu component cluster was strongly blocked (~-5dB) around the peak of platform movement in Motion-Stop and Motion-Go events. A sharp negative was found in the central midline component cluster only in Motion-Deviation events. We believe that these two features were induced by kinesthetic stimuli.

4.1 Mu Components

Mu rhythm is an EEG rhythm recorded usually from the motor cortex of the dominant hemisphere. It is a variant of normality, and it can be suppressed by a simple motor activity, or passively moved [6, 34, 35].

Deviation events involved subject responses to steer the vehicle back to the cruising position. Thus it is expected that mu power would be blocked following deviation events. Our results showed unexpected strong mu blocking in response to Motion-Stop and Motion-Go events in which no action was involved, suggesting kinesthetic stimuli could also induce mu blocking.

Following deviation events, mu power was strongly blocked in both motion and motionless conditions. We found the latency of mu blocking in Motion-Deviation events would lead that in Motionless-Deviation events by a comparable length. Mu blocking thus appeared associated with kinesthetic stimuli delivered to the drivers. In short, long-lasting mu blocking following deviation events began with the EEG brain dynamics induced by kinesthetic stimuli, followed by marked mu power decrease associated with subject motor actions.

4.2 Central Midline Components

The central midline component cluster exhibits a sharp negativity in averaged ERP following Motion-Deviations, but the negativity is missing from the ERP following Motionless-Deviations.

The sharp negativity in the ERP of the central midline component cluster is also consistent with previous VESTEP studies of Elidan et al. [36-38]. They showed a negative potential near Cz or forehead, induced by external kinesthetic stimulus. However, they did not report any mu blocking in response to the kinesthetic stimuli. To the best of our knowledge, this finding had never been reported in the past.

4.3 Alpha Activity and Drowsiness

Traditionally, the EEG alpha band was used as an indicator of drowsiness estimation during driving [12-14]. The alpha power had been reported to index the level of drowsiness in attention-sustained experiments in a laboratory setting. In this study, our results showed that alpha-band activity varies during driving, especially when the vehicle was moving and delivered kinesthetic stimuli to the drivers and passengers, which might confound the fatigue-related alpha power changes in driving. Thus, more care must be taken to examine the validity of using alpha power to index drowsiness level in real driving.

References

1. Elidan, J., Leibner, E., Freeman, S., Sela, M., Nitzan, M., Sohmer, H.: Short and middle latency vestibular evoked responses to acceleration in man. Electroencephalogr Clin. Neurophysiol 80, 140–145 (1991)
2. Baudonniere, P.M., Belkhenchir, S., Lepecq, J.C., Mertz S.: Otolithvestibular-evoked potentials in humans. Intensity, direction of acceleration (Z+, Z-), and BESA modeling of generators. Ann NY Acad Sci. Vol. 871, pp. 384–386 (1999)
3. Probst, T., Dabrowski, H., Liebler, G., Wist, E.: MARDER – Multi-Axes Rotation Device for Experimental Research: a new concept for investigations of the vestibular, oculomotor, and visual systems of humans in three-dimensional space. J. Neuroscience Methods 49, 49–61 (1993)
4. Probst, T., Bablok, E., Dabrowski, H., Dombrowski, J.H., Loose, R., Wist, E.R.: Position and velocity responses from the otoliths and the canals: results from ESA's parabolic flights. Aviat Space Environ Med. 67, 633–639 (1996)
5. Probst, T., Ayan, T., Loose, R., Skrandies, W.: Electrophysiological evidence for direction-specific rotary evoked potentials in human subjects – a topographical study. Neurosci Lett. 239, 97–100 (1997)
6. Loose, R., Probst, T., Tucha, O., Bablok, E., Aschenbrenner, S., Lange, K.W.: Vestibular evoked potentials from the vertical semicircular canals in humans evoked by roll-axis rotation in microgravity and under 1-G. Behavioural Brain Research 134, 131–137 (2002)
7. Kemeny, A., Panerai, F.: Evaluating perception in driving simulation experiments. TRENDS in Cognitive Sciences 7, 31–37 (2003)
8. Wierville, W.W., Casali, J.G., Repa, B.S.: Driver steering reaction time to abrupt-onset crosswind, as measured in a moving-base driving simulator. Hum. Factors 25(1), 103–116 (1983)
9. Reymond, G., Kemeny, A., Droulez, J., Berthoz, A.: Role of lateral acceleration in curve driving: driver model and experiments on a real vehicle and a driving simulator. Hum. Factors. 43, 483–495 (2001)
10. Page, N.G., Gresty, M.A.: Motorist's vestibular disorientation syndrome. J. Neurol. Neurosurg. Psychiatry 48, 729–735 (1985)
11. Groen, E.L., Howard, I.P., Cheung, B.: Influence of body roll on visually induced sensation of self-tilt and rotation. Perception 28, 287–297 (1999)
12. Lin, C.T., Wu, R.C., Jung, T.P., Liang, S.F., Huang, T.Y.: Estimating Driving Performance Based on EEG Spectrum Analysis. EURASIP Journal on Applied Signal Processing 19, 3165–3174 (2005)
13. Lin, C.T., Wu, R.C., Liang, S.F., Chao, W.H., Chen, Y.J., Jung, T.P.: EEG-based drowsiness estimation for safety driving using independent component analysis. IEEE Transactions on Circuits and Systems I. 52, 2726–2738 (2005)

14. Eoh, H.-J., Chung, M.-K., Kim, S.-H.: Electroencephalographic study of drowsiness in simulated driving with sleep deprivation. International Journal of Industrial Ergonomics 35, 307–320 (2005)
15. Stewart, D.: A platform with six degrees of freedom. Proc. Instn Mech. Engr. 180, 371–386 (1965)
16. Reymond, G., Kemeny, A.: Motion cueing in the Renault driving simulator. Veh. Syst. Dynam. 34, 249–259 (2000)
17. Jutten, C., Herault, C.: Blind separation of sources I. An adaptive algorithm based on neuromimetic architecture. Signal Process 24, 1–10 (1991)
18. Comon, P.: Independent component analysis – A new concept? Signal Processing 36, 287–314 (1994)
19. Bell, A.J., Sejnowski, T.J.: An information-maximization approach to blind separation and blind deconvolution. Neural Computation 7, 1129–1159 (1995)
20. Girolami, M.: An alternative perspective on adaptive independent component analysis. Neural Computation 10, 2103–2114 (1998)
21. Lee, T.W., Girolami, M., Sejnowski, T.J.: Independent component analysis using an extended infomax algorithm for mixed sub- and super-Gaussian sources. Neural Computation 11, 606–633 (1999)
22. Jung, T.P., Humphries, C., Lee, T.W., Makeig, S., McKeown, M.J., Iragui, V., Sejnowski, T.J.: Extended ICA removes artifacts from electroencephalographic recordings. Advances in Neural Information Processing Systems 10, 894–900 (1998)
23. Jung, T.P., Makeig, S., Humphries, C., Lee, T.W., McKeown, M.J., Iragui, V., Sejnowski, T.J.: Removing electroencephalographic artifacts by blind source separation. Psychophysiology 37, 163–178 (2000)
24. Jung, T.P., Makeig, S., Westerfield, W., Townsend, J., Courchesne, E., Sejnowski, T.J.: Analysis and visualization of single-trial event-related potentials. Human Brain Mapping 14, 166–185 (2001)
25. Yamazaki, A., Tajima, T., Matsuoka, K.: Convolutive independent component analysis of EEG data. Annual Conference on SICE 2, 1227–1231 (2003)
26. Meyer-Base, A., Auer, D., Wismueller, A.: Topographic independent component analysis for fMRI signal detection. In: Proceedings of the International Joint Conference on Neural Networks. Vol. 1, pp. 601–605 (2003)
27. Naganawa, M., Kimura, Y., Ishii, K., Oda, K., Ishiwata, K., Matani, A.: Extraction of a plasma time-activity curve from dynamic brain pet images based on independent component analysis. IEEE Transactions on Biomedical Engineering 52, 201–210 (2005)
28. Liao, R., Krolik, J.L., McKeown, M.J.: An information-theoretic criterion for intrasubject alignment of FMRI time series: motion corrected independent component analysis. IEEE Transactions on Medical Imaging 24, 29–44 (2005)
29. Makeig, S., Delorme, A., Westerfield, M., Jung, T.-P., Townsend, J., Courchense, E., Sejnowski, T.: Electroencephalographic brain dynamics following visual targets requiring manual responses. PLoS Biology 2(6), 747–762 (2004)
30. Makeig, S.: Auditory event-related dynamics of the EEG spectrum and effects of exposure to tones. Electroencephalography and Clinical Neurophysiology 86, 283–293 (1993)
31. Courchesne, E., Hillyard, S.A., Galambos, R.: Stimulus novelty, task relevance and the visual evoked potential in man. Electroencephalogr Clin. Neurophysiol 39, 131–143 (1975)
32. Polich, J., Comerchero, M.: P3a from visual stimuli: typicality, task, and topography. Brain Topogr 15, 141–152 (2003)

33. Kuhlman, N.W.: Functional topography of the human mu rhythm. Electroencephalography and Clinical Neurophysiology 44, 83–93 (1978)
34. Thilo, K.V., Kleinschmidt, A., Gresty, M.A.: Perception of self-motion from peripheral optokinetic stimulation suppresses visual evoked responses to central stimuli. Journal of Neurophysiology 90, 723–730 (2003)
35. Parker, D.E., Phillips, J.O.: Self-motion perception: assessment by real-time computer-generated animations. Applied Ergonomics 32, 31–38 (2001)
36. Elidan, J., Sohmer, H., Nizan, M.: Recording of short latency vestibular evoked potentials to acceleration in rats by means of skin electrodes. Electroencephalogr Clin. Neurophysiol 53, 501–505 (1982)
37. Elidan, J., Sohmer, H., Lev, S., Gay, I.: Short latency vestibular evoked response to acceleration stimuli recorded by skin electrodes. Annual of Otolrhinollaryngol 93, 257–261 (1984)
38. Elidan, J., Langhofer, L., Honrubia, V.: Recording of short-latency vestibular evoked potentials induced by acceleration impulses in experimental animals: current status of the method and its applications. Electroencephalogr Clin. Neurophysiol 68, 58–69 (1987)